

# Dark-State Optical Potential Barriers with Nanoscale Spacing

Wenchao Ge<sup>1</sup> and M. Suhail Zubairy<sup>1</sup>

<sup>1</sup>*Institute for Quantum Science and Engineering (IQSE) and Department of Physics and Astronomy, Texas A&M University, College Station, TX 77843-4242, USA*

(Dated: August 14, 2019)

Optical potentials have been a versatile tool for the study of atomic motions and many-body interactions in cold atoms. Recently, optical subwavelength single barriers were proposed to enhance the atomic interaction energy scale, which is based on non-adiabatic corrections to Born-Oppenheimer potentials. Here we present a study for creating a new landscape of non-adiabatic potentials—multiple barriers with subwavelength spacing at tens of nanometers. To realize these potentials, spatially rapid-varying dark states of atomic  $\Lambda$ -configurations are formed by controlling the spatial intensities of the driving lasers. As an application, we show that bound states of two and three atoms via magnetic dipolar interactions with weak magnetic moments can be realized in our scheme. Imperfections and experimental realizations of the multiple barriers are also discussed.

## I. Introduction

Optical potentials have been a very useful tool for manipulation of atomic motions, such as simulation of many-body physics [1, 2]. The typical potentials can be generated using a far-detuned light through optical dipole force due to a spatial varying AC-Stark shift [3]. The potential landscape is determined therefore by the spatial variation of the light intensity. Except operating near the surface [4–9] or using special masks [10, 11], the spatial intensity variation is often limited by the wavelength  $\lambda$  of the light. To realize subwavelength resolution in the far field, various approaches have been proposed [12–33], such as multi-tone dressing [18–20], multi-photon process [21–24], and atomic dark states in  $\Lambda$ -configurations [25–33].

Recently, a novel idea of subwavelength optical potentials was proposed by considering the non-adiabatic corrections [34] to the spatially varying dark states in the  $\Lambda$  configurations [35, 36]. A subwavelength potential barrier arises when the kinetic energy of an atom experiences a rapid change of its internal state in a subwavelength region. This new type of optical potentials is drastically different from the optical dipole potentials as the former is purely quantum mechanical since the potential energy is proportional to  $\hbar$ . The first experiment of these barriers has been demonstrated [37]. By using standing-waves, the potentials can form lattices with subwavelength barriers spaced by  $\lambda/2$ . With time-dependent engineering of the lattices, smaller spacings between narrow barriers are possible [38, 39]. However, heating can arise and the dark-state lifetime can be limited due to lattice modulation [39].

In this paper, we present a method to create multi-barrier non-adiabatic potentials with subwavelength spacing, realizing a new type of optical potential landscape without time-dependent modulations. Our idea is based on dark-state non-adiabatic potentials of three-level atoms in the  $\Lambda$  configurations (Fig. 1 (a)) by controlling the spatial intensity variations on the driving lasers. We employ the Born-Oppenheimer (BO) approximation [34] to study the internal eigenstates of the atoms and non-adiabatic corrections from the atomic motions, separately. Our results show that double barriers and triple barriers with subwavelength spacings can be realized.

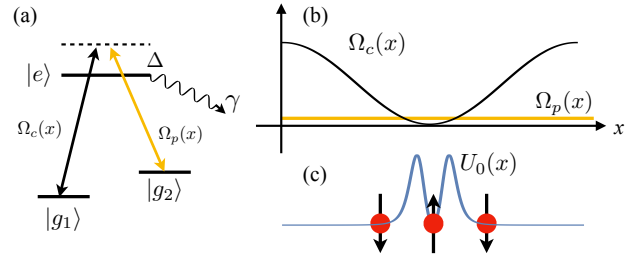


FIG. 1. Schematic of our scheme. (a) Atomic configuration and the coupling to two lasers. An example of (b) spatial dependences for  $\Omega_c(x)$  and  $\Omega_p(x)$  and (c) the corresponding non-adiabatic potential. The circular disks represent atoms and the arrows represent the population of the dark-state atoms.

Moreover, the barrier heights, the spacings, and the number of barriers can be controlled by the amplitude and the phase of the lasers.

Double barrier potentials have been widely studied in solid-state systems, such as semiconductor heterostructures [40–42]. They are important for understanding effects such as resonant tunneling [41] and quasi-bound states [43]. Our scheme offers a new platform to study double barriers for cold atoms in the subwavelength regime, where many-body atomic interactions can be strongly enhanced. As an example, we illustrate the formation of bound states of two and three atoms via magnetic dipolar interactions in these double barriers.

## II. Dark-state trapping and non-adiabatic potentials

We consider three-level atoms with a  $\Lambda$  energy structure shown in Fig. 1 (a). The two ground states  $|g_1\rangle$  and  $|g_2\rangle$  are long-lived, which can be hyperfine-split metastable states or Zeeman sublevels [44], and an excited state  $|e\rangle$  has a spontaneous decay rate  $\gamma$ . The total Hamiltonian of the system includes the kinetic energy and the internal atomic interaction is given by [35]  $\mathcal{H} = \frac{p^2}{2m} + \mathcal{H}_{\text{in}}$ , and the internal Hamiltonian

is

$$\mathcal{H}_{\text{in}} = -\hbar\Delta |e\rangle\langle e| + \left[ \hbar \frac{\Omega_c(x)}{2} |e\rangle\langle g_1| + \hbar \frac{\Omega_p(x)}{2} |e\rangle\langle g_2| + \text{H.c.} \right], \quad (1)$$

where  $\Omega_c(x)$  ( $\Omega_p(x)$ ) is the spatial-dependent Rabi frequency of the off-resonant coupling (probe) field for the transition between  $|e\rangle$  and  $|g_1\rangle$  ( $|g_2\rangle$ ) with a detuning  $\Delta$ . These fields form a resonant Raman transition between the ground states [45]. To study the non-adiabatic corrections, we will employ a similar procedure to that in Ref. [36]. However, in contrast to the previous works [35–39], we consider both the coupling and the probe fields to be position dependent, which will lead to a more general expression of the non-adiabatic corrections shown below.

We are interested in the limit of slow atomic motions such that the energy of the external motion (the kinetic energy and the potential) is much smaller than the internal energy scale determined by  $\mathcal{H}_{\text{in}}$ . Within this limit, we can apply the BO approximation [34] to treat the internal Hamiltonian separately. The validity of this limit will be discussed later. We can diagonalize  $\mathcal{H}_{\text{in}}$  and obtain the eigenstates to be

$$\begin{aligned} |D(x)\rangle &= \frac{-\Omega_p(x)|g_1\rangle + \Omega_c(x)|g_2\rangle}{\Omega(x)}, \\ |B_{\pm}(x)\rangle &= \frac{\Omega_c(x)|g_1\rangle + \Omega_p(x)|g_2\rangle + \Omega_{\pm}(x)|e\rangle}{\sqrt{\Omega^2(x) + \Omega_{\pm}^2(x)}}, \end{aligned} \quad (2)$$

where the corresponding eigenenergies are 0 and  $\hbar\Omega_{\pm}/2$ , respectively. Here  $\Omega(x) = \sqrt{\Omega_c^2(x) + \Omega_p^2(x)}$ ,  $\Omega_{\pm}(x) = -\Delta \pm \sqrt{\Omega^2(x) + \Delta^2}$ . Therefore, the atoms are trapped at the spatial varying dark state  $|D(x)\rangle$  and are decoupled from the laser fields [26–29].

Since the momentum  $p$  and the position  $x$  do not commute, additional contributions arise when we diagonalize the kinetic energy using the position-dependent eigenbasis, which are termed as non-adiabatic corrections or geometric potentials [35, 36]. To see this, we consider the unitary operator [36]

$$\mathcal{R} = |D(x)\rangle\langle D_0| + |B_+(x)\rangle\langle B_{+0}| + |B_-(x)\rangle\langle B_{-0}|, \quad (3)$$

where  $|D_0\rangle$  and  $|B_{\pm 0}\rangle$  are the eigenstates located at a fixed position  $x_0$ . By applying the transformation, we obtain

$$\tilde{\mathcal{H}} = \mathcal{R}^\dagger \mathcal{H} \mathcal{R} = \frac{(p - \mathcal{A})^2}{2m} + \sum_{a=\pm} \hbar \frac{\Omega_a(x)}{2} |B_{a0}\rangle\langle B_{a0}|, \quad (4)$$

where the effective vector potential is given by

$$\begin{aligned} \mathcal{A} &= i\hbar \mathcal{R}^\dagger \partial_x \mathcal{R} \\ &= i\hbar \alpha'(x) \sum_{a=\pm} N_a (|B_{a0}\rangle\langle D_0| - |D_0\rangle\langle B_{a0}|) \\ &\quad + i\hbar \frac{\Omega'(x)}{\Omega(x)} C (|B_{-0}\rangle\langle B_{+0}| - |B_{+0}\rangle\langle B_{-0}|), \end{aligned} \quad (5)$$

with  $\alpha(x) = \arctan[\Omega_p(x)/\Omega_c(x)]$ ,  $N_{\pm} = 1/\sqrt{1 + \Omega_{\pm}^2(x)/\Omega^2(x)}$  and  $C = (\Delta\Omega/2)/(\Delta^2 + \Omega^2)$ . Therefore, we arrive at

$$\begin{aligned} \tilde{\mathcal{H}} &= \frac{p^2}{2m} + U_0(x) |D_0\rangle\langle D_0| \\ &\quad + \sum_{a=\pm} \left( \hbar \frac{\Omega_a(x)}{2} + U_a(x) \right) |B_{a0}\rangle\langle B_{a0}| + \mathcal{V}, \end{aligned} \quad (6)$$

where the non-adiabatic potential for the dark state is [35]

$$U_0(x) = \frac{\hbar^2}{2m} [\alpha'(x)]^2. \quad (7)$$

It is the nonzero derivative of  $\alpha(x)$  that gives rise to potential barriers (positive potential) for the dark state  $|D(x)\rangle$ . Thus the ratio of the two driving lasers, defined as  $f(x) = \Omega_c(x)/\Omega_p(x) = \tan[\alpha(x)]$ , plays an important role in engineering interesting spatial structures of subwavelength barriers. The non-adiabatic potentials for the bright states are

$$\begin{aligned} U_a &= \hbar^2/(2m) [N_a^2 \alpha'^2(x) + C^2 \Omega^2(x)/\Omega^2(x)] \\ &= N_a^2 U_0(x) + 4C^2 U_1(x) \\ &\leq U_0(x) + U_1(x), \end{aligned} \quad (8)$$

where  $U_1(x) = \hbar^2/(8m)\Omega'^2(x)/\Omega^2(x)$ . The off-diagonal contribution that couples between the eigenstates is given by

$$\mathcal{V} = -\frac{p\mathcal{A}}{2m} + U_b(x) |B_{+0}\rangle\langle B_{-0}| + \sum_{a=\pm} U_{0a}(x) |D_0\rangle\langle B_{a0}| + \text{h.c.}, \quad (9)$$

where  $U_b(x) = \hbar^2/(2m)N_+N_- \alpha'^2(x)$ , and  $U_{0a} = \pm N_{\mp} C \alpha'(x) \Omega'(x)/\Omega(x)$ . The coupling strength of  $\mathcal{V}$  is on the order of  $U_i(x)$  ( $i = 0, 1$ ) since  $U_b(x) \leq U_0(x)/2$  and  $|U_{0\pm}(x)| \leq U_{\pm}(x)/2 \leq U_0(x)/2 + U_1(x)/2$ . To ensure the validity of BO approximation, therefore we require

$$U_i(x)/\hbar \ll |\Omega_{\pm}(x)| \quad (i = 0, 1). \quad (10)$$

In particular, as shown numerically in Fig. 2 (b),  $U_1(x) \leq U_0(x)$  around the double barriers. For  $|\Delta| \lesssim |\Omega(x)|$ , we can reduce the above requirement to  $U_0(x) \ll \hbar|\Omega(x)|$ . Under this condition, the off-diagonal coupling  $\mathcal{V}$  is far-detuned from the energy spacing between the eigenstates, therefore it can be treated as a perturbation, which we discuss in the Sec. V A.

In summary, we have derived a general set of expressions of non-adiabatic corrections for an arbitrary spatial function  $f(x) = \Omega_c(x)/\Omega_p(x)$ . Below we show a few concrete examples of  $f(x)$  in generating non-adiabatic potentials of multiple barriers with subwavelength spacings.

### III. Subwavelength optical potentials

The non-adiabatic potential arises due to the rapidly spatial change of the internal dark state. Previous studies [35–39, 46] have focused on the situation when the ratio of the coupling

laser to the driving laser to be an approximated linear function near certain values, which lead to a single potential barrier. Here we consider a more general situation of laser intensities as

$$f(x) \equiv \frac{\Omega_c(x)}{\Omega_p(x)} = \frac{a + b \cos(kx)}{c + d \cos(kx + \phi)}, \quad (11)$$

which can be formed by a combination of standing waves and propagating waves. Here  $a$ ,  $b$ ,  $c$ ,  $d$ , are the amplitude coefficients to be determined and  $\phi$  is the additional phase control.

### A. Single Barrier

Before presenting our results on realizing subwavelength multiple barriers, we briefly review the main result obtained using  $f(x) \approx kx/\epsilon$  for  $|kx| \lesssim \epsilon$  [35–37]. So the non-adiabatic potential for the dark state is given by [36]

$$U_0(x) = \frac{\hbar^2 k^2}{2m\epsilon^2} \frac{1}{[1 + (kx/\epsilon)^2]^2}, \quad (12)$$

which shows a potential barrier located at  $x = 0$  with  $U_0(0) = \frac{\hbar^2 k^2}{2m\epsilon^2}$  and a width  $\Delta x \sim \epsilon/k$ . In general,  $f(x)$  can be made periodic, e.g.  $f(x) = \sin(kx)/\epsilon$  [35, 37], so the separation between two barriers is  $\lambda/2$ . Recent studies show that the separation can be reduced further via Floquet engineering [38, 39].

### B. Double Barrier with subwavelength spacing

Next we study spatial engineering of the Rabi frequencies to realize non-adiabatic multiple barriers with subwavelength spacing. The basic idea is to design a spatial function  $f(x)$  such that its derivative is zero at  $x = x_{\min}$ , but it quickly reaches its maximum in a subwavelength region away from  $x_{\min}$ .

First, we consider the situation for generating double barriers. Specifically, the ratio of the Rabi frequencies is chosen to be

$$f(x) = \frac{1}{\epsilon} \frac{1 + \cos(kx)}{1 + d \cos(kx)}, \quad (13)$$

where  $d < 1$ . Here we take  $\Omega_c(x) = \Omega_0 [1 + \cos(kx)]$  and  $\Omega_p(x) = \Omega_0 \epsilon [1 + d \cos(kx)]$ . We find that the potential features are prominent at  $kx \sim \pi$  and we arrive at

$$\alpha'(x) \approx \frac{k}{\epsilon(1-d)} \frac{k\delta x}{1 + \left[ \frac{k^2 \delta x^2}{2\epsilon(1-d)} \right]^2}, \quad (14)$$

where  $\delta x = x - \pi/k$ . The spatial function of the non-adiabatic potential  $U_0(x)$  can be obtained from Eq. (7) by substituting the above relation of  $\alpha'(x)$ , from which we obtain three important features of the potential:

- (1)  $U_0(x_{\min}) = 0$  with  $x_{\min} = \pi/k$ ;
- (2) two barrier peaks located around  $x_{\max} = \pi/k \pm (4/3)^{1/4} \frac{\sqrt{\epsilon(1-d)}}{k}$  with  $U_0(x_{\max}) = \frac{\hbar^2 k^2}{2m} \frac{\sqrt{27}}{8\epsilon(1-d)}$ ;

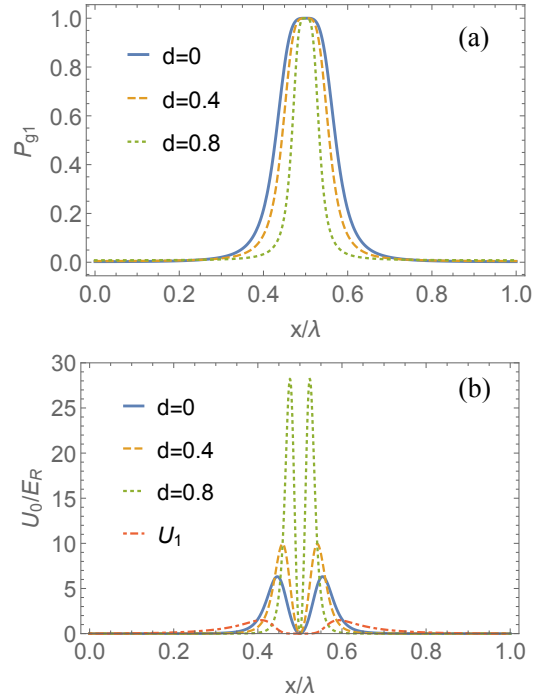


FIG. 2. (a) Dark-state population of  $|g_1\rangle$  for double-barrier potentials as a function of  $x/\lambda$  in one period, and (b) the corresponding non-adiabatic potentials of double barriers with subwavelength spacings for different values of  $d$  at  $\epsilon = 1/10$ . A component of the non-adiabatic potential for the bright states ( $U_1$ , the dot-dashed curve) is plotted in (b) for  $d = 0$ .

(3) based on the first two, we get a non-adiabatic potential well with a subwavelength width at half maximum to be  $\Delta x \approx 0.2 \sqrt{\epsilon(1-d)}\lambda$ .

Furthermore, we study spatial variation on the population of one of the ground states, e.g.  $P_{g_1}(x) = \frac{1}{1+f^2(x)}$  (see Fig. 2 (a)). The non-adiabatic potential  $U_0(x) \propto (\partial P_{g_1}(x)/\partial x)^2$ , meaning that it is due to the rapid change of the population as a function of position such that the atoms can not adjust its internal state adiabatically. In particular,  $\partial P_{g_1}(x)/\partial x \propto f'(x) = 0$  at  $x = k/\pi$ , which corresponds to the dip in the non-adiabatic potential.

The double-barrier potential  $U_0(x)$  for different values of  $d$  is plotted in Fig. 2 (b) using the full expression derived from Eq. (13). The aforementioned features agree well with the numerical results. In particular, we find that the peak value  $U_0(x_{\max}) \propto 1/(\epsilon(1-d))$  and the subwavelength size  $\Delta x \propto \sqrt{\epsilon(1-d)}$ , which are less sharply dependent on  $\epsilon$  than those in the single potential barriers, where  $U_0(x_{\max}) \propto 1/\epsilon^2$  and  $\Delta x \propto \epsilon$  [35, 36]. However, we have an additional factor  $1-d$ , which can be controlled to make the potentials more prominent.

In addition, we note that for any function  $f(x) \approx (x - x_{\min})^n/\epsilon$  for  $n > 1$  (intergers), the corresponding geometric potential can be a double barrier centered at  $x = x_{\min}$  since  $f'(x_{\min}) = 0$ . Therefore, we provide a simple realization of non-adiabatic potential double barriers, making them drastically different from those in the case of  $f(x) \approx x/\epsilon$  [35–

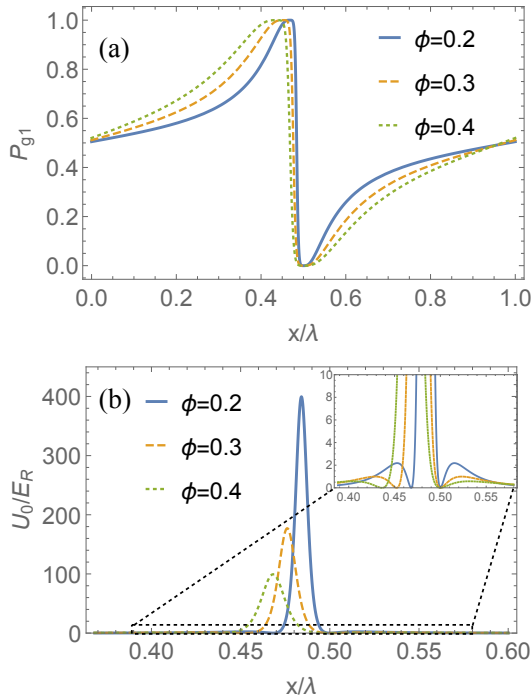


FIG. 3. (a) Dark-state population of  $|g_1\rangle$  for creating triple-barrier potentials as a function of  $x/\lambda$ , and (b) the corresponding non-adiabatic potentials of triple barriers with subwavelength spacings for different values of  $\phi$ . The inset magnifies the dashed-box area to show the triple-barrier feature.

[37, 46]. Moreover, our method does not require lattice modulation [38, 39] or atomic levels with multi- $\Lambda$  configurations [29, 35].

### C. Multiple Barrier with subwavelength spacing

As another example, we would like to show that by tuning the spatial function of  $f(x)$ , we can also realize a three-peak non-adiabatic potential, which forms a double well with a large barrier in the middle. To see this, we consider the spatial function

$$f(x) = \frac{1 + \cos(kx)}{1 + \cos(kx + \phi)}, \quad (15)$$

where  $\Omega_c(x) = \Omega_0 [1 + \cos(kx)]$  and  $\Omega_p(x) = \Omega_0 [1 + \cos(kx + \phi)]$ . Here the only control parameter is the phase  $\phi$ . We derive

$$\alpha'(x) = k \frac{\sin(kx + \phi) - \sin kx + \sin \phi}{(1 + \cos kx)^2 + (1 + \cos(kx + \phi))^2}. \quad (16)$$

By examining the properties of  $\alpha'(x)$ , we find the spatial features of  $U_0(x)$  as follows:

- (1) A central peak at  $x_c = \frac{\pi}{k} - \frac{\phi}{2k}$  with  $U_0(x_c) = \frac{8\hbar^2 k^2}{m\phi^2}$ ;
- (2) Two dips at  $x_{\min} = x_c \pm \frac{\phi}{2k}$  with  $U_0(x_{\min}) = 0$ ;
- (3) Two lower peaks at maximum at  $x_{\max} = x_c \pm \frac{\phi}{k}$  with  $U_0(x_{\max}) = \frac{9\hbar^2 k^2}{200m\phi^2}$ .

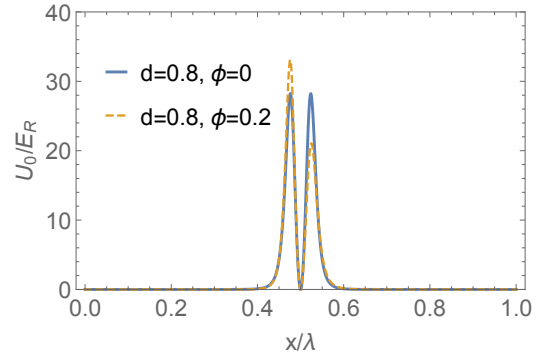


FIG. 4. Tuning the barrier height in non-adiabatic double barriers for otherwise the same parameters as in Fig. 2.

We plot both the ground-state population  $P_{g_1}$  and the geometric potential  $U_0(x)$  as a function of  $x$  for different values of  $\phi$  in Fig. 3. Two flat regions in the population correspond to the dips in  $U_0(x)$  and the large slope corresponds to the central peak in  $U_0(x)$ .

We note that the double-well potential looks similar to the plot in the right-upper panel in Fig. 3 (b) in Ref. [37], but they are of different natures. Here the potential is a characteristic of the spatial varying Rabi frequencies and the state is complete dark, while the one in Ref. [37] is due to the off-resonant Raman lasers so that the resulting potential is not complete dark.

### D. Additional Tunability

In addition to tuning the separation of non-adiabatic barriers to form potential wells, we can also tune the heights of those barriers simultaneously. For example, by considering

$$f(x) = \frac{1}{\epsilon} \frac{1 + \cos(kx)}{1 + d \cos(kx + \phi)}, \quad (17)$$

We can change the symmetric double barriers into asymmetric (see Fig. 4).

The non-adiabatic multiple barriers are important in two ways. First, they provide a new subwavelength potential landscape. Quasi-bound states and resonant tunnelings of multi-barrier potentials can be studied using Wentzel-Kramers-Brillouin (WKB) approximation [47, 48]. The potentials can also form multi-barrier lattices since  $f(x)$  has a period of  $\lambda$ , thus they are useful for the study of band structures, and even trapping atoms through the quasi-bound states. Second, the subwavelength features of the multiple barriers may permit the study of enhanced dipole-dipole interactions between atoms.

## IV. Application: bound states

We now discuss a study of many-body physics permitted by the non-adiabatic potential barriers. The spatial-varying

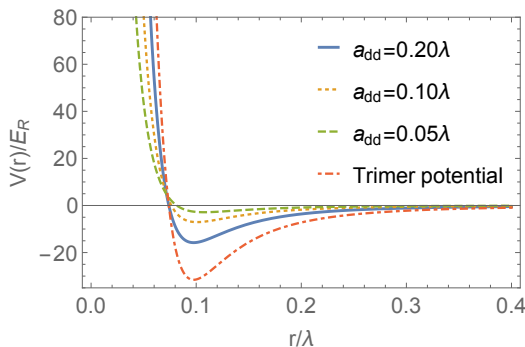


FIG. 5. Total potential energy of two atoms under the double-barrier potential with  $d = 0$ ,  $\epsilon = 1/10$  at different dipolar lengths. The dot-dashed curve is the total potential energy of three atoms for otherwise the same parameters as the solid curve ( $a_{dd} = 0.20\lambda$ ).

dark state may allow the atoms to have spatially dependent magnetic moments [2]. The subwavelength feature allows us to study strong magnetic dipole-dipole interactions between atoms in the potential. For concreteness, we assume the magnetic moments are aligned perpendicular to  $x$ -axis that the atoms are located at. The strength of the magnetic moment of an atom is taken to be  $\mu(x) = m[2P_{g_1}(x) - 1]$ , which depends on the state (spin) of the atom, i.e.,  $P_{g_1}(x)$ . For the situation of two atoms, the total Hamiltonian is given by [35]

$$\mathcal{H}_{MB} = \frac{p_1^2}{2m} + \frac{p_2^2}{2m} + U_0(x_1) + U_0(x_2) + \frac{\mu_0\mu(x_1)\mu(x_2)}{4\pi|x_1 - x_2|^3}, \quad (18)$$

where  $\mu_0$  is the vacuum permeability, and  $x_i$  and  $p_i$  are the position and the momentum of the  $i$ th atom.

In the case of the double barriers, the atoms repel each other through the magnetic dipolar interaction if they both stay in the well. Thus a bound state can not be formed. Instead, a bound state can be formed if only one atom sits inside the well. The condition for the bound state is  $E_{\min} + \frac{\mu_0\mu(x_1)\mu(x_2)}{4\pi|x_1 - x_2|^3} < 0$ , where  $E_{\min}$  is the minimum energy of the atom inside the potential well and the energy (kinetic and geometric potential) of the other atom outside the well is neglected. By considering the size of the potential well and using the uncertainty principle, we estimate  $E_{\min} \approx \hbar^2 k^2 / [2m\epsilon(1-d)]$ . Then we estimate the minimum magnetic moment in order to form a bound state. Since the magnetic dipole moments are close to  $\pm\mu$  inside and outside the well, the required dipolar length  $a_{dd} \equiv \mu_0\mu^2 m / (12\pi\hbar^2)$  [49] is on the order of the typical subwavelength spacing, i.e.,  $a_{dd} \gtrsim 0.2\sqrt{\epsilon(1-d)}\lambda \sim \Delta x$ . This is useful for the study of magnetic dipole-dipole interactions, where the magnetic moment is usually very weak [49]. The analytical result is further confirmed with the numerical results using the total potential  $V(|x_1 - x_2|) = U_0(x_1) + U_0(x_2) + \frac{\mu_0\mu(x_1)\mu(x_2)}{4\pi|x_1 - x_2|^3}$  by assuming  $x_1 = x_{\min}$  plotted in Fig. 5. Moreover, the double-barrier potential can lead to bound states of three atoms known as trimers. Our trimer has one atom inside the well and two outside on each side of the barrier. Due to the trimer configuration (Fig. 1 (c)), its binding energy is stronger than that of the dimer by comparing the solid and the dot-dashed curves

in Fig. 5. In the above analysis, the contact interaction due to  $s$ -wave scattering [49] is neglected.

Similarly, bound states can be formed in the case of the triple potential barriers. The atoms attract each other if they are separated by the center barrier such that the dipoles are opposite and the magnitude is about  $\mu$  (Fig. 3). The attractive dipolar force will balance with the large potential barrier between the wells to form a dimer. With periodic potentials, our multiple barriers can be interesting for the study of many-body physics in band structures, which is out of the scope of this work.

## V. Practical Considerations

### A. Imperfections

The dark states is uncoupled from the driver lasers, thus it is less prone to spontaneous emission. The main imperfection come from the off-resonant non-adiabatic coupling to the open channels given by  $\mathcal{V}$  in Eq. (9). The off-resonant non-adiabatic coupling leads to population in the open channels given by  $P_B$  and scattering of the atom through the spontaneous emission of the excited state [36] with a rate  $\gamma_d$ .

For  $U_0(x) \ll \hbar|\Omega(x)|$ , the excitation to the open channels can be estimated perturbatively [45] as  $P_B \sim |\langle B_{a0} | \mathcal{V} | D_0 \rangle|^2 / \Omega^2(x) \lesssim E_{\min}^2 / \hbar^2 \Omega^2(x) \ll 1$ . The effective scattering rate of the dark state is given by  $\gamma_d \sim \gamma E_{\min}^2 / \hbar^2 \Omega^2(x)$  for bound states. A more rigorous result of the dark-state decay rate is calculated from the corrections to the dispersion of atoms in the Bloch bands [35], which shows a similar relation to our perturbative result.

### B. Experimental Implementations

The non-adiabatic potential multiple barriers require the  $\Lambda$  atomic configuration and spatial control on the Rabi frequencies. The  $\Lambda$  atomic configurations have been frequently used in electromagnetic-induced transparency [44] and coherent population transfer [50]. The first experiment on non-adiabatic potentials has been performed using an ultracold  $^{171}\text{Yb}$  gas [37] with hyperfine-split ground states.

The spatial dependence of the Rabi frequencies  $\Omega_c(x)$  and  $\Omega_p(x)$  is of the form  $a + b\cos(kx)$ , which can be realized by superposing a standing-wave and a propagating wave derived from the same laser. Thus, the spatial function  $f(x)$  is insensitive to the laser intensity fluctuation. As the perfect spatial function may be challenge in experiment, a double barrier can be more easily demonstrated with an approximated function  $f(x) = (x - x_{\min})^2 / \epsilon$  by shaping the coupling and the probe lasers.

We can determine the minimum barrier spacing from  $U_0(x) \ll \hbar|\Omega(x)|$ . The minimum value of the Rabi frequency is  $\Omega(x) = \sqrt{\Omega_c^2(x) + \Omega_p^2(x)} \approx \Omega_0\epsilon(1-d)$  for the double-barrier potentials, and  $\Omega(x) \approx \Omega_0[1 - \cos^2(\phi)] \approx \Omega_0\phi^2/2$  for the triple-barrier potentials. Considering  $\Omega_0 = 2\pi \times 100$  MHz,

$\lambda = 532$  nm, and  $U_0(x) \leq \hbar|\Omega(x)|/5$  for  $^{171}\text{Yb}$  atoms, we obtain the minimum barrier spacing to be 13 nm and 24 nm for the double-barrier potentials and the triple-barrier potentials, respectively. The corresponding minimum energy inside the double barriers is  $E_{\min}/\hbar \approx 2\pi \times 280$  kHz. We estimate the maximum excitation probability is  $P_B \approx 4\%$ . Taking  $\gamma = 2\pi \times 182$  kHz [37], we find the scattering rate on the dark states through the open channel is about  $2\pi \times 7$  kHz. In the above analysis, we assumed  $|\Delta| \lesssim |\Omega(x)|$ , however, for larger single-photon detunings, the laser intensities need to be stronger in order to get the same subwavelength feature without breaking the BO approximations.

## VI. Conclusion

In this work, we presented a method of creating non-adiabatic potentials of multiple barriers separated at tens of

nanometers via spatial engineering of the laser intensities. General formulae of non-adiabatic corrections were derived and the validity of the Born-Oppenheimer approximation was discussed. We studied several concrete examples on realizing subwavelength multiple barriers and their application for bound states.

The multi-barrier potentials can be a new platform for the study of many-body interactions in cold atoms enhanced by the subwavelength features. This scheme may also allow further studies on trapping atoms without the conventional optical dipole potentials and super-resolution quantum microscopy [51, 52].

## Acknowledgments

This research is supported by a grant from King Abdulaziz City for Science and Technology (KACST)

- 
- [1] I. Bloch, *Nature Physics* **1**, 23 (2005).  
 [2] I. Bloch, J. Dalibard, and W. Zwerger, *Reviews of Modern Physics* **80**, 885 (2008).  
 [3] R. Grimm, M. Weidemüller, Y. B. Ovchinnikov, B. Bederson, and H. Walther, “Optical dipole traps for neutral atoms,” in *Advances In Atomic, Molecular, and Optical Physics*, Vol. 42 (Academic Press, 2000) pp. 95–170.  
 [4] D. E. Chang, J. D. Thompson, H. Park, V. Vuletić, A. S. Zibrov, P. Zoller, and M. D. Lukin, *Physical Review Letters* **103**, 123004 (2009).  
 [5] M. Gullans, T. G. Tiecke, D. E. Chang, J. Feist, J. D. Thompson, J. I. Cirac, P. Zoller, and M. D. Lukin, *Physical Review Letters* **109**, 235309 (2012).  
 [6] O. Romero-Isart, C. Navau, A. Sanchez, P. Zoller, and J. I. Cirac, *Physical Review Letters* **111**, 145304 (2013).  
 [7] J. D. Thompson, T. G. Tiecke, N. P. de Leon, J. Feist, A. V. Akimov, M. Gullans, A. S. Zibrov, V. Vuletić, and M. D. Lukin, *Science* **340**, 1202 (2013).  
 [8] R. Mitsch, C. Sayrin, B. Albrecht, P. Schneeweiss, and A. Rauschenbeutel, *Nature Communications* **5**, 5713 EP (2014).  
 [9] A. González-Tudela, C. L. Hung, D. E. Chang, J. I. Cirac, and H. J. Kimble, *Nature Photonics* **9**, 320 EP (2015).  
 [10] B. Brezger, T. Schulze, P. O. Schmidt, R. M. T. Pfau, and J. Mlynek, *Europhysics Letters (EPL)*, **46**, 148 (1999).  
 [11] F. M. Huang and N. I. Zheludev, *Nano Letters*, **Nano Letters **9**, 1249 (2009).  
 [12] J. R. Gardner, M. L. Marable, G. R. Welch, and J. E. Thomas, *Physical Review Letters* **70**, 3404 (1993).  
 [13] Y. Qi, F. Zhou, T. Huang, Y. Niu, and S. Gong, *Journal of Modern Optics*, *Journal of Modern Optics* **59**, 1092 (2012).  
 [14] D. D. Yavuz, N. A. Proite, and J. T. Green, *Physical Review A* **79**, 055401 (2009).  
 [15] Z. Liao, M. Al-Amri, and M. Suhail Zubairy, *Physical Review Letters* **105**, 183601 (2010).  
 [16] Q. Sun, M. Al-Amri, M. O. Scully, and M. S. Zubairy, *Physical Review A* **83**, 063818 (2011).  
 [17] S. Nascimbene, N. Goldman, N. R. Cooper, and J. Dalibard, *Physical Review Letters* **115**, 140401 (2015).  
 [18] W. Yi, A. J. Daley, G. Pupillo, and P. Zoller, *New Journal of Physics*, **10**, 073015 (2008).  
 [19] N. Lundblad, P. J. Lee, I. B. Spielman, B. L. Brown, W. D. Phillips, and J. V. Porto, *Physical Review Letters* **100**, 150401 (2008).  
 [20] M. Shotton, D. Trypogeorgos, and C. Foot, *Physical Review A* **78**, 051602 (2008).  
 [21] P. R. Berman, B. Dubetsky, and J. L. Cohen, *Physical Review A* **58**, 4801 (1998).  
 [22] M. Weitz, G. Cennini, G. Ritt, and C. Geckeler, *Physical Review A* **70**, 043414 (2004).  
 [23] T. Salger, C. Geckeler, S. Kling, and M. Weitz, *Physical Review Letters* **99**, 190405 (2007).  
 [24] W. Ge, P. R. Hemmer, and M. S. Zubairy, *Physical Review A* **87**, 023818 (2013).  
 [25] M. Sahr, H. Tajalli, K. T. Kapale, and M. S. Zubairy, *Physical Review A* **72**, 013820 (2005).  
 [26] G. S. Agarwal and K. T. Kapale, *Journal of Physics B: Atomic, Molecular and Optical Physics*, **39**, 3437 (2006).  
 [27] D. D. Yavuz and N. A. Proite, *Physical Review A* **76**, 041802 (2007).  
 [28] A. V. Gorshkov, L. Jiang, M. Greiner, P. Zoller, and M. D. Lukin, *Physical Review Letters* **100**, 093005 (2008).  
 [29] M. Kiffner, J. Evers, and M. S. Zubairy, *Physical Review Letters* **100**, 073602 (2008).  
 [30] H. Li, V. A. Sautenkov, M. M. Kash, A. V. Sokolov, G. R. Welch, Y. V. Rostovtsev, M. S. Zubairy, and M. O. Scully, *Physical Review A* **78**, 013803 (2008).  
 [31] J. Mompert, V. Ahufinger, and G. Birkl, *Physical Review A* **79**, 053638 (2009).  
 [32] D. Viscor, J. L. Rubio, G. Birkl, J. Mompert, and V. Ahufinger, *Physical Review A* **86**, 063409 (2012).  
 [33] J. A. Miles, Z. J. Simmons, and D. D. Yavuz, *Physical Review X* **3**, 031014 (2013).  
 [34] R. Dum and M. Olshanii, *Physical Review Letters* **76**, 1788 (1996).  
 [35] M. Lacki, M. A. Baranov, H. Pichler, and P. Zoller, *Physical Review Letters* **117**, 233001 (2016).  
 [36] F. Jendrzejewski, S. Eckel, T. G. Tiecke, G. Juzeliūnas, G. K. Campbell, L. Jiang, and A. V. Gorshkov, *Physical Review A* **94**, 063422 (2016).**

- [37] Y. Wang, S. Subhankar, P. Bienias, M. Lacki, T.-C. Tsui, M. A. Baranov, A. V. Gorshkov, P. Zoller, J. V. Porto, and S. L. Rolston, *Physical Review Letters* **120**, 083601 (2018).
- [38] S. Subhankar, P. Bienias, P. Titum, T. Tsui, Y. Wang, A. Gorshkov, S. Rolston, and J. Porto, arXiv preprint arXiv:1906.07646 (2019).
- [39] M. Lacki, P. Zoller, and M. Baranov, arXiv preprint arXiv:1906.07649 (2019).
- [40] V. J. Goldman, D. C. Tsui, and J. E. Cunningham, *Physical Review B* **36**, 7635 (1987).
- [41] A. G. Petukhov, A. N. Chantis, and D. O. Demchenko, *Physical Review Letters* **89**, 107205 (2002).
- [42] R. Songmuang, G. Katsaros, E. Monroy, P. Spathis, C. Bougerol, M. Mongillo, and S. De Franceschi, *Nano Letters*, *Nano Letters* **10**, 3545 (2010).
- [43] H. C. Nguyen, M. T. Hoang, and V. L. Nguyen, *Physical Review B* **79**, 035411 (2009).
- [44] M. Fleischhauer, A. Imamoglu, and J. P. Marangos, *Reviews of Modern Physics* **77**, 633 (2005).
- [45] M. O. Scully and M. S. Zubairy, *Quantum optics* (Cambridge University Press, 1999).
- [46] P. Bienias, S. Subhankar, Y. Wang, T. Tsui, F. Jendrzejewski, T. Tiecke, G. Juzeliunas, L. Jiang, S. Rolston, J. Porto, *et al.*, arXiv preprint arXiv:1808.02487 (2018).
- [47] A. Modinos and N. Nicolaou, *Surface Science* **17**, 359 (1969).
- [48] A. Dutt and S. Kar, *American Journal of Physics*, *American Journal of Physics* **78**, 1352 (2010).
- [49] T. Lahaye, C. Menotti, L. Santos, M. Lewenstein, and T. Pfau, *Reports on Progress in Physics*, **72**, 126401 (2009).
- [50] K. Bergmann, H. Theuer, and B. W. Shore, *Reviews of Modern Physics* **70**, 1003 (1998).
- [51] M. McDonald, J. Trisnadi, K.-X. Yao, and C. Chin, *Physical Review X* **9**, 021001 (2019).
- [52] S. Subhankar, Y. Wang, T.-C. Tsui, S. L. Rolston, and J. V. Porto, *Physical Review X* **9**, 021002 (2019).